IOPscience iopscience.iop.org

Home Search Collections Journals About Contact us My IOPscience

Effects of measurement noise on modal parameter identification

This article has been downloaded from IOPscience. Please scroll down to see the full text article.

2012 Smart Mater. Struct. 21 065008

(http://iopscience.iop.org/0964-1726/21/6/065008)

View the table of contents for this issue, or go to the journal homepage for more

Download details:
IP Address: 71.175.184.72
The article was downloaded on 22/05/2012 at 02:52

Please note that terms and conditions apply.

IOP Publishing Smart Materials and Structures
Smart Mater. Struct. **21** (2012) 065008 (15pp) doi:10.1088/0964-1726/21/6/065008

Effects of measurement noise on modal parameter identification

S Dorvash and S N Pakzad

Department of Civil and Environmental Engineering, Lehigh University, Bethlehem, PA, USA

E-mail: dorvash@lehigh.edu

Received 19 February 2012, in final form 5 April 2012
Published 18 May 2012
Online at stacks.iop.org/SMS/21/065008

Abstract
In the past decade, much research has been conducted on data-driven structural health monitoring (SHM) algorithms with use of sensor measurements. A fundamental step in this SHM application is to identify the dynamic characteristics of structures. Despite the significant efforts devoted to development and enhancement of the modal parameter identification algorithms, there are still substantial uncertainties in the results obtained in real-life deployments. One of the sources of uncertainties in the results is the existence of noise in the measurement data. Depending on the subsequent application of the system identification, the level of uncertainty in the results and, consequently, the level of noise contamination can be very important. As an effort towards understanding the effect of measurement noise on the modal identification, this paper presents parameters that quantify the effects of measurement noise on the modal identification process and determine their influence on the accuracy of results. The performance of these parameters is validated by a numerically simulated example. They are then used to investigate the accuracy of identified modal properties of the Golden Gate Bridge using ambient data collected by wireless sensors. The vibration monitoring tests of the Golden Gate Bridge provided two synchronized data sets collected by two different sensor types. The influence of the sensor noise level on the accuracy of results is investigated throughout this work and it is shown that high quality sensors provide more accurate results as the physical contribution of response in their measured data is significantly higher. Additionally, higher purity and consistency of modal parameters, identified by higher quality sensors, is observed in the results.

(Some figures may appear in colour only in the online journal)

1. Introduction

Identification of dynamic characteristics of constructed structures is one of the fundamental steps in many structural health monitoring applications. Having dynamic properties enables assessment of a structure's performance, calibration of finite element models, and assists with the maintenance of the structure over its life time. In practice, dynamic characteristics of constructed structures are obtained through vibration monitoring tests and applying system identification algorithms on the measured data. Over the past three decades, vibration monitoring techniques have improved from several points of view, from advanced instrumentation technology to enhanced data processing and system identification algorithms. The objectives of the improvements in vibration monitoring fall into three basic categories: (i) enhancing the accuracy of the estimated results, (ii) minimizing the cost, and (iii) simplicity of the implementation.

One of the distinguished improvements introduced to vibration monitoring systems is deployment of wireless technology for data communication in a sensing network. This approach was first introduced to structural health monitoring (SHM) applications in the late 1990s (Straser and Kiremidjian 1998) and showed its inherent potential in improving the monitoring techniques in terms of cost and deployment (Lynch *et al* 2003). As the advantages of wireless sensor networks (WSNs) became evident, researchers developed different WSN platforms and deployed them in SHM systems

 © 2012 IOP Publishing Ltd Printed in the UK & the USA

(Tanner *et al* 2003, Lynch *et al* 2004, Chung *et al* 2004, Lynch *et al* 2005, Pakzad *et al* 2008, Whelan and Janoyan 2009, Kim *et al* 2010, Jang *et al* 2010). While researchers have shown the effective role of WSNs in improving the affordability of vibration monitoring (ease of implementation and reduction of costs), their possible impact on the reliability and accuracy of the results is still a research question.

Fundamental factors affecting the performance of a vibration monitoring system are (i) software characteristics—the implemented data processing techniques and procedures—and (ii) hardware characteristics—the monitoring system including sensors and data acquisition system (e.g. the embedded analog filters, analog-to-digital converters, etc).

Perhaps the most significant distinction between WSNs and their traditional counterparts, wired systems, is the wireless communication which is the objective of their invention. However, some challenges in the design of wireless sensor units, such as the trade-off between functionality and power consumption, and also attempts to minimize the cost, will cause limitations in their architecture which do not necessarily exist in the design of wired systems. Although a large number of wireless sensing unit prototypes with different embedded sensors and filters has been presented in the literature (Lynch 2006), the number of commercially available platforms with integrated quality sensors is limited. Therefore, it is important to carefully investigate the impact of sensor quality on modal identification results.

As the source of measurement noise, the selected sensors may introduce an epistemic uncertainty into the results of system identification (Moon 2006). Depending on the subsequent application of the system identification (e.g. damage detection, finite element model updating, etc) the level of uncertainty in the results can be very important. On the other hand, despite the development of numerous system identification methods and many successful implementations on structural systems (Juang and Pappa 1985, Pandit 1991, James *et al* 1992, Overschee and Moor 1994, Roeck *et al* 1995, Farrar and James 1997), relatively limited effort has been devoted to evaluation of the results in terms of accuracy and credibility. Even the limited research is mainly concerned with the uncertainties associated with environmental and operational conditions (Peeters and De Roeck 2001a, 2001b, Sohn 2007), excitation characteristics (Reynders *et al* 2007, Kijewski-Correa and Pirnia 2007) and data processing methodology (Grimmelsman and Aktan 2005, Reynolds *et al* 2004), and less attention is paid to the impact of the measurement system and the possible uncertainties derived from measurement noise. The lack of research on the effects of uncertainties on system identification results is even more critical in the area of large-scale structural monitoring, where many different sources of noise exist.

A major challenge in such studies is that the existing accuracy indicators in modal identification are mostly relative indicators which are useful when comparing different identified parameters. For example, Juang and Pappa (1985) introduced two parameters (modal amplitude coherence and modal phase collinearity) that can be utilized to determine the confidence level of each identified modal parameter when the eigensystem realization algorithm (ERA) is used. Although these parameters are very helpful in selecting structural modes and eliminating the spurious modes, they cannot indicate the general performance of the whole sensing system. However, it will be beneficial to use them to compare the performance of two sensing systems in terms of accuracy of results. In this paper, parameters to investigate the effect of sensing quality are presented and the impact of measurement noise on vibration monitoring is discussed through a field example.

1.1. Scope of the paper

This study evaluates the influence of measurement system quality on modal parameter estimation, using the ERA–NExT algorithm. The physical contribution ratio is introduced, which reflects the level of contribution of physical modes in the estimation of impulse response versus noise and computational modes when ERA–NExT is used. The parameter is validated through implementation on a numerically simulated example. Additionally, the developed parameter is implemented on data collected from vibration monitoring of the Golden Gate Bridge which was performed by Pakzad *et al* (2008), using a wireless sensor network. The sensor boards in this vibration monitoring test utilized two types of accelerometer with low and high characteristic noise levels to measure a broad range of ambient vibrations. The performance of the two sensing systems in estimation of the Golden Gate Bridge's modal parameters is examined and the results are presented. The modal phase collinearity (MPC) and modal amplitude coherence (MAC), developed by Pappa *et al* (1993), are also used for investigating the accuracy and purity of each modal parameter identified by both sensing networks. Furthermore, the consistency of the identified modal parameters through the increase of model order in ERA–NExT is evaluated and the results of different sensing systems are compared and discussed.

2. Modal identification using ERA–NExT

In this section the basic formulations of the natural excitation technique (NExT) and the eigensystem realization algorithm (ERA) are presented to provide background and terminology for derivation of physical contribution ratios later in this paper.

2.1. The natural excitation technique

The natural excitation technique (NExT) is an approach to modal testing which allows structures to be tested in their ambient environments (James *et al* 1993). The fundamental idea of this approach is that the cross-correlation function between two measured displacements (or accelerations) of a structure satisfies the homogeneous differential equation of motion (Caicedo *et al* 2004). Consider the equation of motion for a multi-degree-of-freedom, linear time invariant system:

$$M\ddot{q}(t) + C\dot{q}(t) + Kq(t) = u(t) \tag{1}$$

where M, C and K are N by N mass, damping and stiffness matrices, $u(t)$ is the input of the system which can be an

external excitation or ground motion, and $\ddot{q}(t)$, $\dot{q}(t)$ and $q(t)$ are acceleration, velocity and displacement responses at time t. Assuming that the excitations are stationary random processes and the structural parameters (M, C and K) are deterministic, equation (1) can be written as

$$M\ddot{R}_{qq_i}(\tau) + C\dot{R}_{qq_i}(\tau) + KR_{qq_i}(\tau) = 0 \tag{2}$$

where $R(.)$ denotes the correlation function. This equation shows that the correlation function of displacement satisfies the homogeneous differential equation of motion. It can be shown that the correlation function of acceleration response also satisfies equation (2) (Beck *et al* 1994). Therefore, for a structural system under ambient vibration (e.g. wind, traffic and ground motions), the free decay response can be estimated by computing the correlation function of its acceleration responses. The estimated free decay function is required in many modal parameter identification algorithms such as ERA (Juang and Pappa 1985) or Polyreference (Vold and Rocklin 1982).

2.2. The eigensystem realization algorithm

One of the effective and commonly used time-domain system identification techniques is the eigensystem realization algorithm (ERA), developed by Juang and Pappa (1985). This method uses the system's impulse response to derive the system's parameters, without considering external force in its formulation. When the ERA is accompanied by the NExT, the impulse response is estimated by the auto- and cross-correlation functions of the measured responses.

Consider the discrete-time state-space representation of the systems

$$x(n+1) = Ax(n) + B_u(n) \tag{3a}$$

$$y(n) = Cx(n) + Du(n) \tag{3b}$$

where $x(n)$ is the state vector at time step n, $y(n)$ is the observation vector at time step n, $u(n)$ is the input, and the system's parameters A, B, C, and D are the discrete-time state, input, output, and feed through matrices, respectively. In the ERA, to estimate the system's parameters the Hankel block data matrix is formed as

$$H(n-1) = \begin{bmatrix} \hat{Y}(n) & \hat{Y}(n+1) & \cdots & \hat{Y}(n+q-1) \\ \hat{Y}(n+1) & \hat{Y}(n+2) & \cdots & \hat{Y}(n+q) \\ \vdots & \vdots & \ddots & \\ \hat{Y}(n+p-1) & \hat{Y}(n+p) & \cdots & \hat{Y}(n+p+q-2) \end{bmatrix} \tag{4}$$

where $\hat{Y}(n)$ is the $N \times N$ (the number of outputs is assumed to be equal to the number of inputs and equal to N) estimated impulse response matrix at the time step n; i.e., $\hat{y}_{ij}(n)$ is the estimated ith output, due to an impulse at the jth input at time step n. p and q correspond to the order of the Hankel matrix. The following relationship between the state matrices and the estimated impulse response can be obtained by substituting the impulse function, as the input, into equations (3*a*) and (3*b*):

$$\hat{Y}(n) = CA^{n-1}B. \tag{5}$$

Therefore, the Hankel matrix is composed of the system's parameters as

$$H(n-1) = \begin{bmatrix} CA^{n-1}B & CA^{n}B & \cdots & CA^{n+q-2}B \\ CA^{n}B & CA^{n+1}B & \cdots & CA^{n+q-1}B \\ \vdots & \vdots & \ddots & \vdots \\ CA^{n+p}B & CA^{n+p+1}B & \cdots & CA^{(n-3)+p+q}B \end{bmatrix}. \tag{6}$$

To extract an estimate of the system's matrices, the Hankel data block matrix, $H(n-1)$, is decomposed using singular-value decomposition (SVD) for $n = 1$:

$$H(0) = P\Sigma Q^{\mathrm{T}} \tag{7}$$

where P and Q^{T} are matrices of left and right singular vectors of $H(0)$ respectively, and Σ is the diagonal matrix of singular values. Small singular values along the diagonal of $\sum$ correspond to computational or noise modes (nonphysical spurious modes). Therefore, the rows and columns associated with nonphysical modes are eliminated from the singular-vector and singular-value matrices. The truncated matrices, $\sum_{\mathrm{n}}$, P_{n} and Q_{n}, are used to estimate the state-space matrices for the discrete-time structural model as follows (Juang and Pappa 1985):

$$\hat{A} = \Sigma_{\mathrm{n}}^{-1/2} P_{\mathrm{n}}^{\mathrm{T}} H(1) Q_{\mathrm{n}} \Sigma_{\mathrm{n}}^{-1/2} \tag{8}$$

$$\hat{B} = \Sigma_{\mathrm{n}}^{1/2} Q_{\mathrm{n}}^{\mathrm{T}} E_{\mathrm{inp}} \tag{9}$$

$$\hat{C} = E_{\mathrm{out}}^{\mathrm{T}} P_{\mathrm{n}} \Sigma_{\mathrm{n}}^{1/2} \tag{10}$$

where E_{inp} and E_{out} are matrices of 1 and 0 with appropriate dimensions based on the sizes of inputs and outputs ([I 0]). Eigenvalue decomposition of the estimated state matrix results in the diagonal matrix of eigenvalues (Λ) and the matrix of eigenvectors (ψ) which are functions of the system's natural frequencies (ω_{n} s), damping ratios (ζ_{n} s) and mode shapes ($\vec{\phi}_{\mathrm{n}}$ s).

3. Contribution ratio of physical modes in measured signals

This section presents the formulation of a parameter, called the physical contribution ratio (PCR), which quantifies the participation of physical modal vibrations in the estimation of impulse response and modal parameters. The performance of this parameter is examined later, through implementation of a numerical example and data collected from ambient vibration tests of the Golden Gate Bridge.

As mentioned earlier, using NExT the impulse response of the structure is estimated and can be used in the ERA or a similar algorithm for modal parameter estimation. The objective is to quantify what portion of this estimated impulse function is driven from physical modal vibration compared to

noise. The portion of the estimated impulse function which is driven from structural modes (PCR) reflects the level of noise contamination in the modal identification process. Considering the measured signal as a combination of the real response and the measurement noise, it can be written as

$$y(t) = q(t) + n_s(t) \tag{11}$$

where $q(t)$ is the structural response and $n_s(t)$ is the stochastic noise in the measurement. The impulse response, $Y(\tau)$, is then estimated by the cross-correlation function of measured response as

$$\hat{Y}(\tau) = R_y(\tau) \tag{12}$$

where R_y is a function of time delay or lag τ. The estimation can be rewritten as

$$\hat{Y}(\tau) = R_{qq}(\tau) + R_{nn}(\tau) + R_{qn}(\tau) + R_{nq}(\tau). \tag{13}$$

Based on the assumption that the measurement noise is uncorrelated with the response of the structure, the last two terms on the right-hand side of equation (13) vanish and the impulse response can be written as

$$\hat{Y}(\tau) = R_{qq}(\tau) + R_{nn}(\tau). \tag{14}$$

Assuming that the noise characteristic is reflected in $R_n(\tau)$, equation (14) shows that the measurement noise has a direct impact on the estimated impulse response. Also, it can be assumed that there is no correlation between measurement noises of different sensors. Thus, mainly the diagonal components of the correlation function are assumed to be contaminated by the measurement noise in the system.

Now that the relation between noise characteristics and the estimated impulse response has been clarified, the next step in correlating the noise effects to the identified modal parameters is to find the relationship between the estimated impulse response and the estimated modal properties. Considering the discrete state-space model, the A, B and C matrices of the system can be estimated based on the estimated impulse response, using the ERA. The relationship between the state matrices and the estimated impulse response follows equation (5). Transforming the system from physical coordinates into modal coordinates ($A^n = \psi \Lambda^n \psi^{-1}$), equation (5) can be written as

$$\hat{Y}(n) = C\psi \Lambda^{n-1} \psi^{-1} B \tag{15}$$

where ψ is the matrix of eigenvectors and Λ is the diagonal matrix of eigenvalues (λ_i s) in discrete form. Also, $C\psi = E_{\text{out}}^{\text{T}} P \Sigma_n^{1/2} \psi$ and $\psi^{-1}B = \psi^{-1} \Sigma_n^{1/2} Q_n^{\text{T}} E_{\text{inp}}$ are mode shapes and modal amplitudes, respectively, which are the outcomes of minimum realization in the ERA. The mode shapes and modal amplitudes can be rewritten as

$$C\psi = [\vec{\phi}_1 \ \cdots \ \vec{\phi}_m] \qquad \text{and} \qquad \psi^{-1}B = \begin{bmatrix} \vec{b}_1 \\ \vdots \\ \vec{b}_m \end{bmatrix}$$

where $\vec{\phi}_1$ to $\vec{\phi}_m$ are column vectors of mode shapes, and $\vec{b}_1$ to $\vec{b}_m$ are row vectors of corresponding modal amplitudes (the modal amplitude of a particular mode when an impulse is applied at different nodes); m is the order of the system or the size of the state vector. It should be noted that the order of the system is usually selected higher than what is minimally required (twice the number of outputs) to reduce the estimation bias, but in the over parameterized model noise and computational spurious modes will also appear.

Expanding the estimated impulse response as sum of m identified modes of the system, it can be written as

$$\hat{Y}(n) = \begin{bmatrix} \vec{\phi}_1 \ \cdots \ \vec{\phi}_m \end{bmatrix} \Lambda^{n-1} \begin{bmatrix} \vec{b}_1 \\ \vdots \\ \vec{b}_m \end{bmatrix} = \begin{bmatrix} \sum_{i=1}^{m} \phi_{1i} b_{i1} \lambda_i^{n-1} & \sum_{i=1}^{m} \phi_{1i} b_{i2} \lambda_i^{n-1} & \cdots & \sum_{i=1}^{m} \phi_{1i} b_{iN} \lambda_i^{n-1} \\ \sum_{i=1}^{m} \phi_{2i} b_{i1} \lambda_i^{n-1} & \sum_{i=1}^{m} \phi_{2i} b_{i2} \lambda_i^{n-1} & & \\ \vdots & & \ddots & \vdots \\ \sum_{i=1}^{m} \phi_{Ni} b_{i1} \lambda_i^{n-1} & \cdots & \cdots & \sum_{i=1}^{m} \phi_{Ni} b_{iN} \lambda_i^{n-1} \end{bmatrix}_{N \times N} \tag{16}$$

where N is the number of outputs and b and ϕ are components of the mode shape and modal amplitude vectors (e.g. ϕ_{ij} is the ith component of the jth mode shape and, similarly, b_{jk} is the jth mode's amplitude at the kth location). This equation presents each component of the estimated impulse response as the summation of contributions of all the estimated modes (in terms of mode shapes, modal amplitudes and eigenvalues). Having this expansion for $\hat{Y}(n)$, the contribution of each mode can be identified. Since the impulse response is a function of time, the PCR parameter is defined by the integration over time (summation in the discrete domain) which is a measure of the signal's power. Therefore, the PCR of the jth mode in the kth diagonal component of the estimated impulse response (auto-correlation function of a signal with the kth node as the reference) is defined as

$$\text{PCR}_{kj} = \frac{\sum_n \phi_{kj} b_{jk} \lambda_j^{n-1}}{\sum_n \sum_{i=1}^{m} \phi_{ki} b_{ik} \lambda_i^{n-1}} \tag{17}$$

where n is the time index.

When the noise contamination is constant for all the modes it is evident that a higher PCR will correspond to less sensitivity of the mode to the noise. In other words, higher amplitude results in higher signal-to-noise ratio in modal coordinates. Therefore, those modes with higher contribution in the auto-correlation function of a particular node are less sensitive to the noise level of the corresponding sensor.

4. Validation of the physical contribution ratio through a simulated example

To validate the performance of the PCR in the presence of measurement noise and also environmental and operational condition changes, a simulated model is developed. The

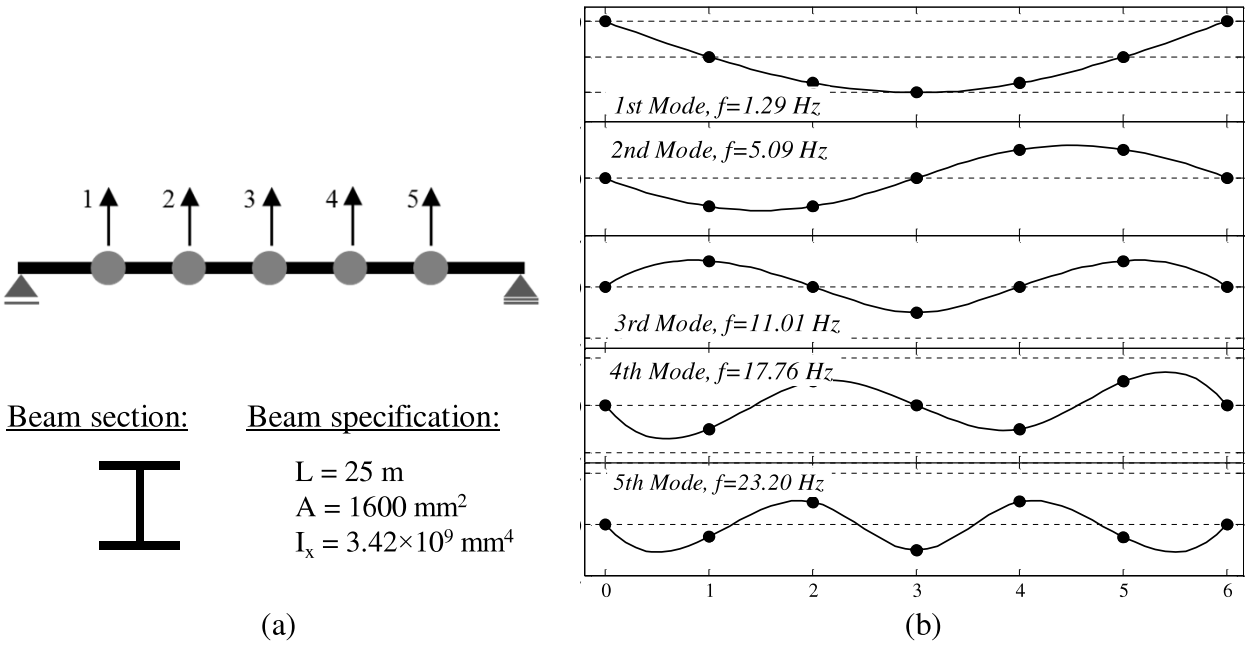

Figure 1. (a) Beam example specifications, (b) identified modal frequencies and modeshapes.

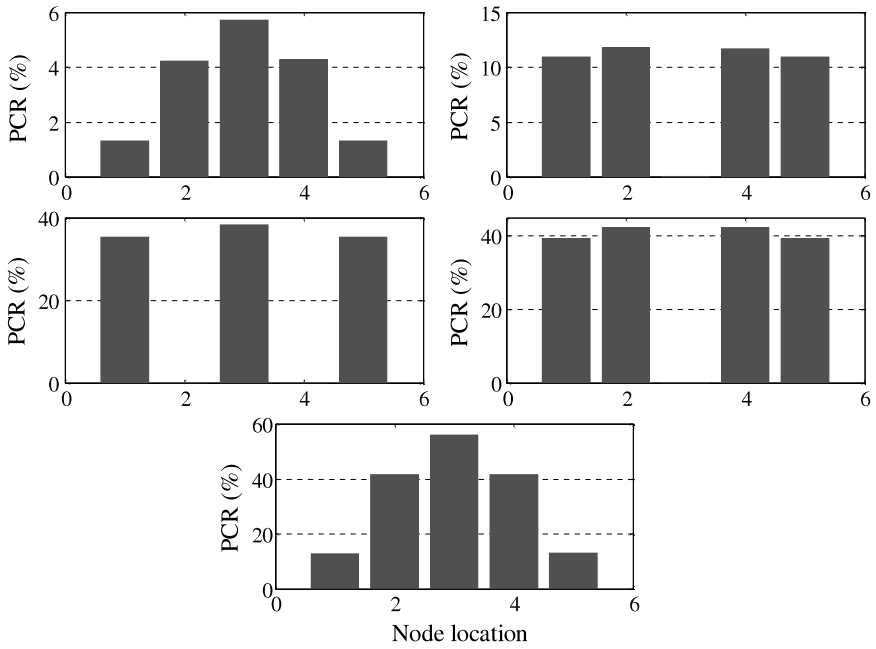

Figure 2. PCR values of different nodes for different modes.

model is a simply supported steel beam with five lumped masses along the span. Figure 1(a) shows the specifications of this beam model. The masses are determined based on the weight of the beam element and an assumed 3 m tributary of 6 kN m^{-2} uniform load. The acceleration response of the beam to random noise at five locations is simulated and used for modal identification process. ERA–NExT with model order ten is selected to extract the five fundamental modes of the beam model. The identified natural frequencies and modeshapes of the beam are shown in the plots of figure 1(b).

The PCR values at different nodes for each of the fundamental modes are computed and presented in figure 2. Comparing these plots with the mode shapes of the bridge, it is evident that the PCRs are proportional to the modal ordinates. However, the PCR also accounts for the modal amplitude factor (b) and the modal frequency, as predicted by equation (17). It can be seen that the PCR value is relatively small in a couple of nodes for some of the vibration modes. These nodes correspond to small (or zero) modal displacement. It is also observed that the PCR is larger for higher modes, which is consistent with the acceleration response's power spectrum for this model. In this example, the amounts of participation of the first and second modes in the acceleration response are small as their angular frequencies

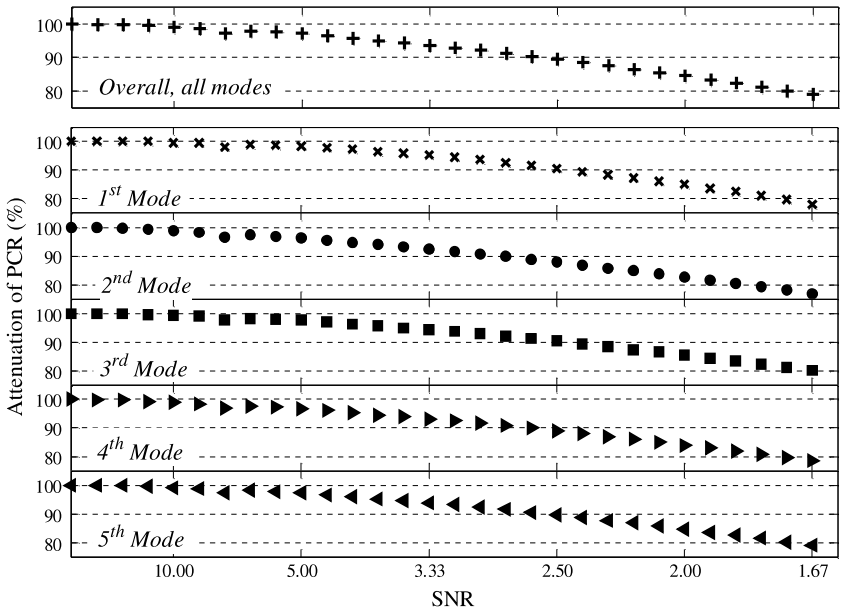

Figure 3. Variation of the PCR values at different nodes due to increase of artificial noise (decrease of SNR).

are less than unity. It is worth noting that the sum of the PCRs at each node over the five natural frequencies is almost 100%. This is obvious as the response is noise-free.

To see the effect of measurement noise on the PCR values, artificial stochastic white noise is added to the acceleration response and the variation of these ratios is inspected as the root mean square (RMS) of noise increases and the signal-to-noise ratio (SNR) decreases. As expected, the noise causes attenuation of the PCR, since it adds into the frequency contents of the measured response at non-fundamental frequencies. This behavior can be clearly observed in figure 3 which shows the PCR for each mode, and also the overall PCR for all modes.

The PCR is developed to reflect the noise contamination of the response which is due to nonphysical variables (e.g. measurement noise). However, to further investigate the performance of the PCR in the presence of environmental and operational changes, its behavior under different structural perturbations is also inspected. For this purpose, the changes in the PCR against random changes in the structural stiffness and also addition of random impulsive loads are evaluated. The stiffness perturbation is to represent the variation of structural properties due to different environmental conditions (e.g. temperature change effects) and the addition of random impulsive loads is to also reflect the existence of non-stationary loads on structures (e.g. random heavy traffic loads). Of course in real world structures many parameters are affected by these types of environmental and operational changes. In this example, however, only the effects of these two factors are considered.

For the stiffness perturbation, the components of the stiffness matrix are subjected to a random change with increasing mean values and the corresponding changes in the PCR are inspected. The results are shown in figure 4 where the PCRs are plotted for each mode and also the summation of all modes versus stiffness perturbation percentages. It can be seen that, in contrast to the noise contamination, the changes in the PCR do not follow any decreasing trend and the overall values (summation of all fundamental modes) are almost 100% for all cases. This is reasonable as the physical changes in the structure only alter the contributions of different modes and do not decrease the overall PCR in the modal estimation process.

A similar process is applied to observe the effects of adding random impulsive loads on the PCR values. The loads are selected based on the possible scenario of a truck passing over a bridge structure. Thus, the loads are applied to different nodes at different times (i.e. a moving load) and their amplitudes are selected as random values with increasing mean up to 30 times the applied stationary load RMS (the maximum impulsive load generates $L/1000$ deflection at the mid-span). The result of PCR variation is plotted in figure 5. It can be seen that the overall PCRs for all modes are almost unchanged as the random impulsive loads increase. The contributions of different modes, however, change due to the increasing impulsive load which is again expected as random impulsive loads may alter the load shape function and, as a result, change the participation of different modes.

Through this numerical example, it is observed that the PCR is sensitive to the level of noise in the measured response. However, the overall value of the PCR (for all modes) is not sensitive to the structural changes (e.g. environmental and operational changes), though its values in different modes change due to changes in modal participation of different modes.

5. Accuracy assessment of the identified modal parameters using the MAC and MPC

In order to validate the identified modal parameters, it is necessary to assess the accuracy of the results, particularly when there are different sources of uncertainty in the vibration data (e.g. environmental affects, measurement noise, etc).

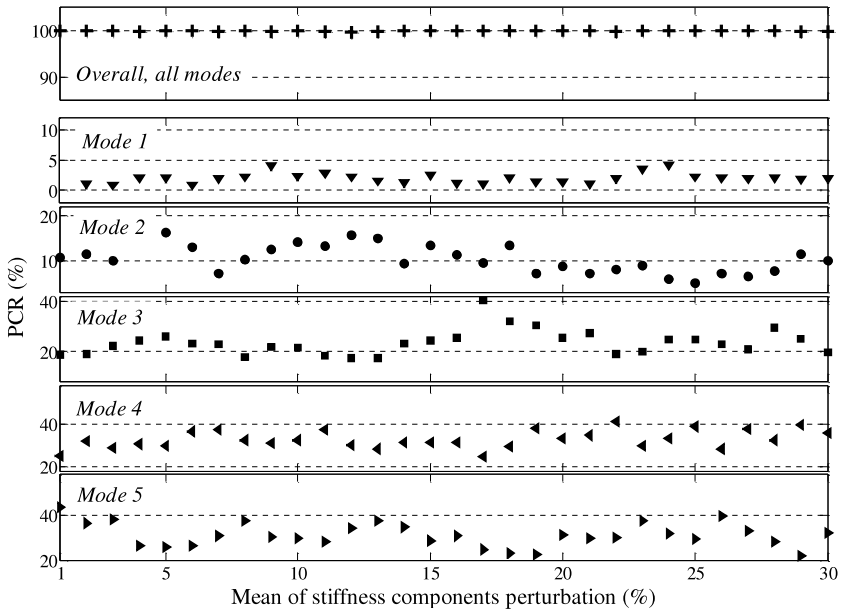

Figure 4. Variation of the PCR due to increasing random perturbation of the stiffness components.

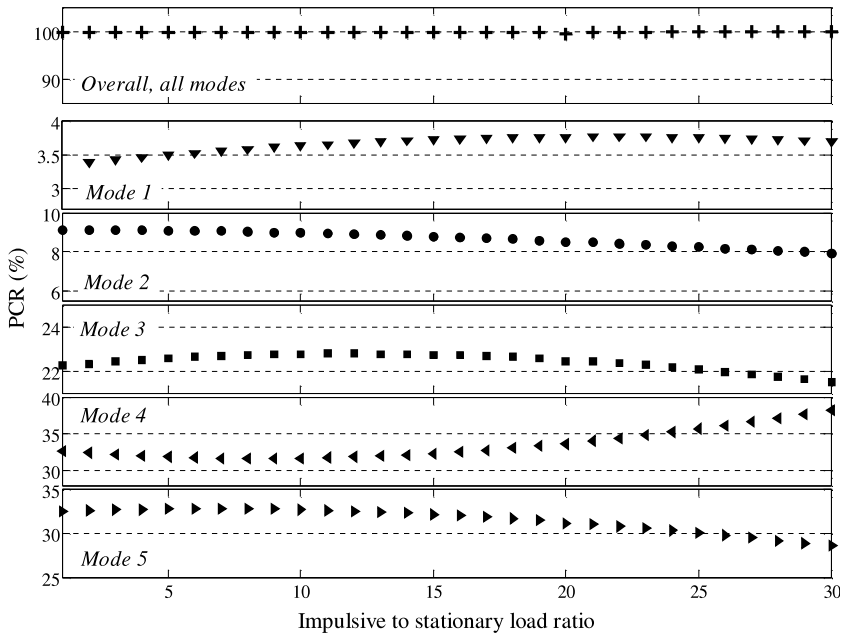

Figure 5. Variation of the PCR values due to an increasing ratio of random impulsive load to the stationary load RMS.

This section focuses on approaches which quantify the uncertainties of each identified mode and provide parameters to measure the accuracy of modal identification results.

A study of the effects of noise on modal identification using ERA was performed by Juang and Pappa (1986), and a mathematical foundation was established for determining the accuracy of identified genuine modes versus those associated with noise. In this study, the modal amplitude coherence (as a special case of degree of the modal purity parameter) is introduced which quantifies the consistency of the identified modes versus time. Another indicator developed also by Juang and Pappa (1985) is the modal phase collinearity (MPC) which measures the strength of the linear functional relationship between the real and imaginary parts of the mode shapes for each identified mode.

5.1. Modal amplitude coherence (MAC)

The modal amplitude coherence is defined as the coherence between the modal amplitude history and the one formed by extrapolating the initial value to later points in time, using the identified eigenvalues. As a result of minimum order realization, the triple $[z, E_p^T P \Sigma_n^{1/2} \psi, \psi^{-1} \Sigma_n^{1/2} Q_n^T E_m]$ is available where z and ψ are eigenvalues and eigenvectors of the A matrix (state matrix). The second element, $E_p^T P \Sigma_n^{1/2} \psi$,

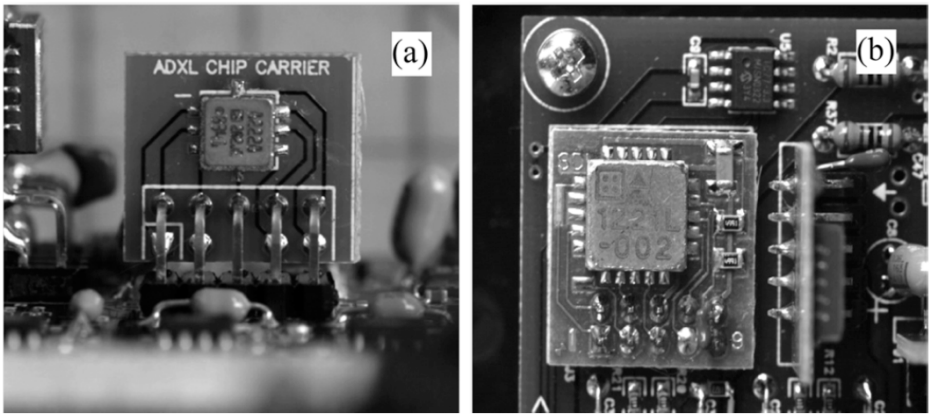

Figure 6. ADXL202 (a) and Silicon Design 1221L (b) accelerometers.

is the matrix of mode shapes and the third element, $\psi^{-1}\Sigma_n^{1/2}Q_n^T E_m$, is called the initial modal amplitude. Having the initial modal amplitudes and the identified eigenvalues, the modal amplitude can be extrapolated. At the same time the counterpart sequence would be the identified modal amplitude time history, obtained from decomposition of the Hankel matrix ($\psi^{-1}\Sigma_n^{1/2}Q_n^T$). Finally, the MAC can be obtained by computing the coherence of the extrapolated and identified modal amplitudes. This parameter takes values between 0 and 1 where values close to 1 indicate that the estimated system eigenvalue and the initial modal amplitude are close to the true system. Also values that are close to zero indicate that the identified mode is a noise-driven mode. This parameter determines the level of the purity of the identified mode in the presence of measurement noise (Juang and Pappa 1985).

5.2. Modal phase collinearity

The modal phase collinearity (MPC) quantifies the spatial consistency of the identified mode shapes. When the modes are normal (which is expected in an ideal lightly damped system) the vibrations of all locations on the structure are either in-phase or out-of-phase with one another (Pappa *et al* 1993). However, in practice, usually the phase angles of the identified modal displacement vectors are not consistent. This behavior is not necessarily due to structural properties (e.g. non-proportional damping), but can be a result of noise in the process. Particularly in lightly damped structures, the modes are normal and the inconsistent phase angles are often the result of poor data quality. The MPC is an indicator which quantifies the collinearity of the phase angle in the identified mode shapes and determines their accuracy. Similarly to the MAC, the MPC values are also ranged from 0 to 1, where 0 indicates uncorrelated phase angles in the identified mode, and 1 represents a perfect in-phase mode.

6. Evaluation of measurement noise effects using Golden Gate Bridge data

In this section the data collected in a deployment of a wireless sensor network on the Golden Gate Bridge is used as an example to apply the PCR, MAC, and MPC parameters for quantification of modal identification accuracy (Pakzad *et al* 2008). The data include measurements by two synchronized sensor networks with different sensor sensitivities. Having two synchronized data sets allows examination of the accuracy parameters in the presence of only uncertainties derived from measurement noise (as the same response with the same environmental and operational conditions is measured by the two sensor types). Therefore, the performances of the sensor types can be compared by comparing the accuracies of the results.

6.1. The wireless sensor network

Pakzad *et al* (2008), Pakzad and Fenves (2009), Pakzad (2010) presented the results of long term ambient vibration monitoring on the Golden Gate Bridge where the acceleration data were measured using a WSN, consisting of 65 sensing units, during a three month deployment period. The sensing units in this network utilized three hardware components: sensors, filters and microcontroller, and a radio for wireless communication. For the measurement of low-level and high-level accelerations, two micro-electro-mechanical system (MEMS) accelerometer sensors were used each in two directions. The use of two accelerometer types in the sensor board design is a cost-effective solution and allows examination of performance–price tradeoffs. Analog Device's ADXL202 was the high-level sensor (figure 6(a)) which provides a ± 2 g range with a sensitivity of 1 mg at 25 Hz (AnalogDevices 1999). For low-level vibrations, Silicon Design 1221L (figure 6(b)) was used which has higher sensitivity and is suitable for ambient structural vibrations (SiliconDesign 2007). The acceleration range of the Silicon Design 1221L accelerometer was reduced from ± 2 to ± 0.15 g to achieve a higher resolution from the 16 bit analog-to-digital converter (ADC). Table 1 shows the detailed specifications of the two accelerometer sensors, integrated in the sensor board.

The measured signal from the MEMS accelerometers was fed to a single-pole anti-aliasing low-pass filter with a cutoff frequency of 25 Hz. The cutoff frequency was high enough to

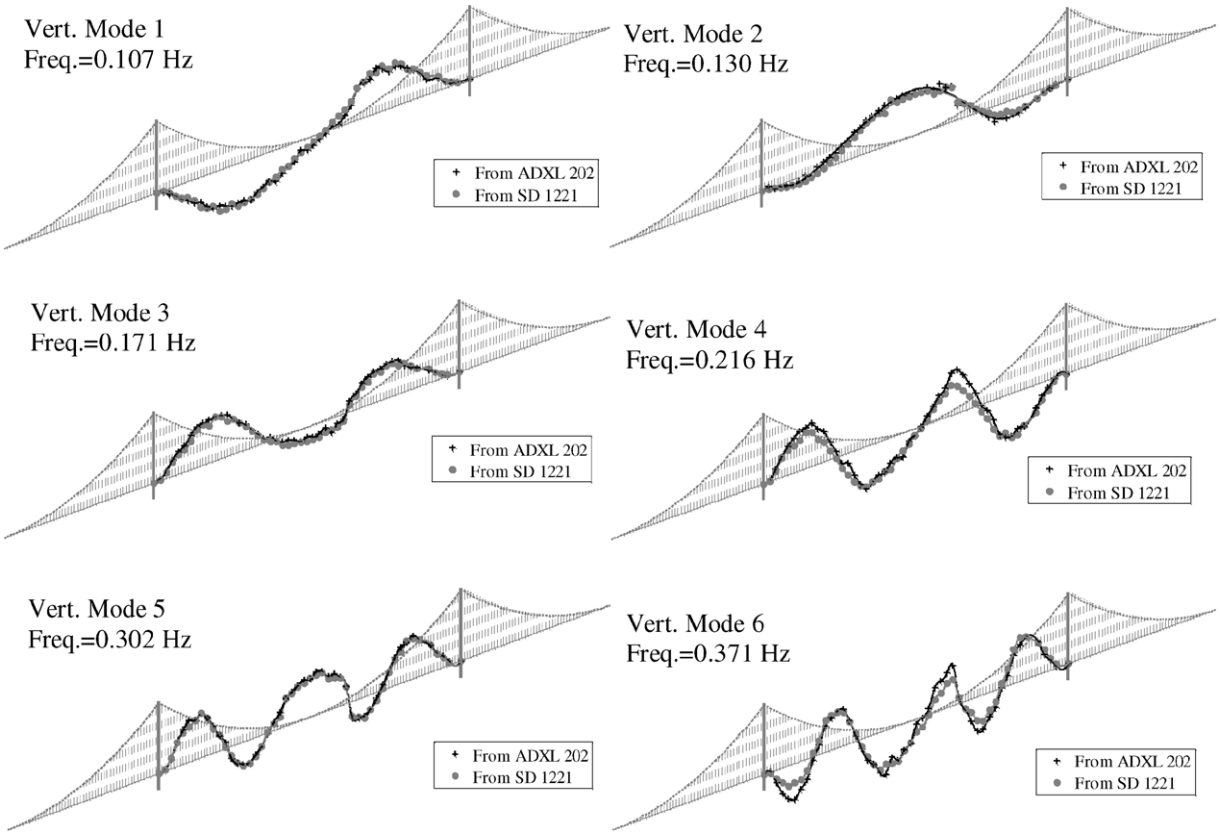

Figure 7. The first six identified vertical modes of the main span of the Golden Gate Bridge.

Table 1. Specifications of the Silicon Design 1221L and ADXL202 accelerometers.

Specification	Silicon design 1221L accelerometer	ADXL202 accelerometer
Acceleration range	± 0.15 g (reduced from ± 2 g)	± 2 g
Frequency response	0–400 Hz	0 to 500 Hz
Nominal output noise	2 μg $(\text{Hz})^{-1/2}$	500 μg $(\text{Hz})^{-1/2}$
Temperature range	-55 to $+125$ °C	-40 to $+85$ °C
Dimensions	$3.5 \times 3.5 \times 1.05$ (mm)	$5 \times 5 \times 2$ (mm)
Cost	~$150 (in 2005)	~$10 (in 2005)

capture many high vibration modes of this long span bridge (Pakzad *et al* 2008). The filtered analog signal was then fed to a 16 bit ADC for each of the channels. The acceleration data were collected with a high-frequency sampling of 1 kHz and were downsampled on-board to 200 Hz to reduce the noise level of the measured signal. For a detailed description of the implemented WSN architecture, the system software, and the full scale deployment on the bridge, the reader is referred to Pakzad (2010).

Before application of the sensor board in vibration monitoring of the Golden Gate Bridge, the sensors were validated through static and dynamic tests, using a reference Wilcoxon 731-4A low-noise piezoelectric accelerometer (Pakzad 2010). The result of the validation showed that the Silicon Design 1221L accelerometer behaves very similarly to the low-noise reference sensor in both time and frequency domains, whereas the ADXL202 sensor presents higher noise in the data, especially in the low-frequency range. Considering the significant difference in the cost ($10 versus $150 in 2005), it is important to evaluate the significance of the lower noise level of the more expensive accelerometer in the modal identification process.

6.2. Identified modal parameters of the Golden Gate Bridge

The data collected by the two accelerometer sensor types from the ambient vibration of the Golden Gate Bridge are used for modal parameter identification of the bridge, using ERA–NExT. A summary of identified natural frequencies and damping ratios of vertical modes resulting from ADXL202 and SD1221L accelerometer data is presented in table 2. Figure 7 also shows the first six identified vertical mode shapes resulting from the two sensor types. More detailed information about the identified modal properties of the Golden Gate Bridge using the ambient vibrations can be found in Pakzad and Fenves (2009).

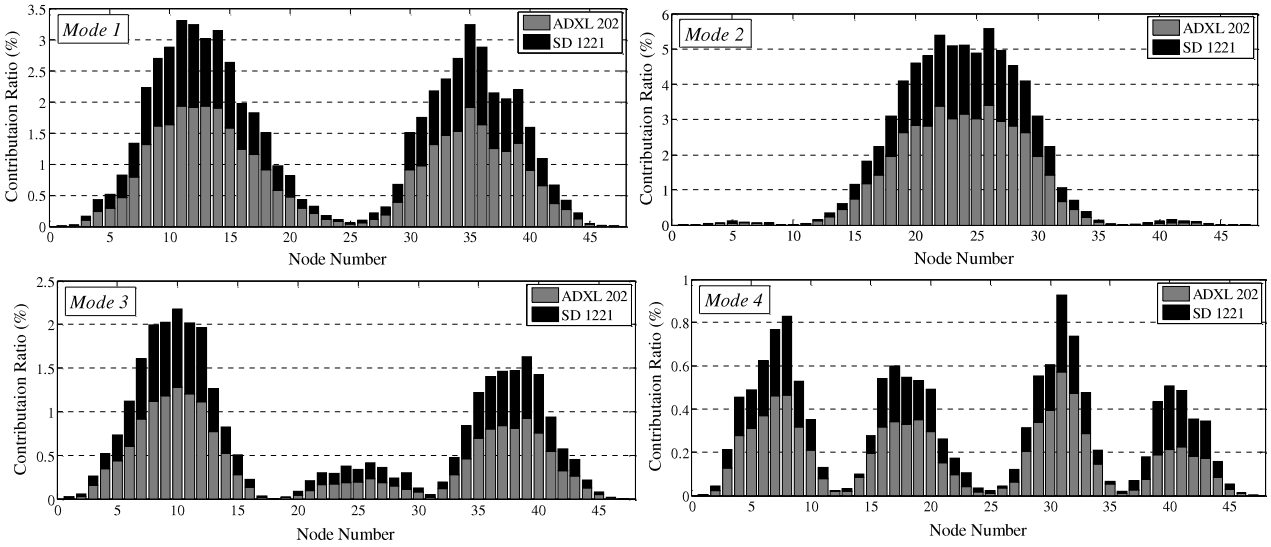

Figure 8. Physical contribution ratios of four identified modes at different nodes.

Table 2. Identified natural frequencies and damping ratios of the vertical modes identified by ERA–NExT, using data collected by ADXL202 and Silicon Design 1221L accelerometers.

	Frequency (Hz)		Damping ratio (%)	
Mode	ADXL202 sensors	SD1221L sensors	ADXL202 sensors	SD1221L sensors
1 A	0.1067	0.1067	2.1031	1.7599
2 S	0.1326	0.1330	2.2178	1.9824
3 S	0.1708	0.1711	1.4182	0.9943
4 A	0.2164	0.2170	2.1239	2.0639
5 S	0.3015	0.3012	1.1098	1.1078
6 A	0.3705	0.3701	1.2066	1.4229
7 S	0.4610	0.4607	0.5531	0.6631
8 A	0.5491	0.5458	2.4465	2.3976
9 S	0.6620	0.6620	0.5082	0.5407
10 A	0.7691	0.7664	0.8779	1.0146
11 S	0.8884	0.8905	0.8451	0.8692
12 A	1.0042	1.0040	1.2559	0.8739
13 S	1.1330	1.1312	0.7320	0.6391
14 A	1.2565	1.2641	0.7099	0.8225
15 A	1.5234	1.5195	0.6339	0.7918
16 S	1.6573	1.6596	0.5997	0.6314
17 A	1.7659	1.7764	0.5260	0.3653
18 S	1.9281	1.9295	0.6840	0.6692
19 A	2.0623	2.0713	0.5221	0.4724
20 S	2.1797	2.1954	0.4829	0.6695
21 A	2.3187	2.3248	0.5614	0.5998
22 A	2.5739	2.5929	0.2970	0.3761
23 S	2.7082	2.7127	0.4910	0.3537
24 A	2.8397	2.8399	0.2722	0.3363
25 A	3.7677	3.7605	0.3257	0.4901

By comparing the modal properties, it is clear that both sensor types are capable of estimating the fundamental modal parameters of the bridge. However, some inconsistencies in the results of the two sensor types, especially in damping ratios and mode shapes, can be observed. Applying PCR, MAC, and MPC parameters on the estimated modal parameters, the performance of the two sensing systems, in terms of accuracy and consistency of results, is investigated.

6.3. Evaluation of the results using the physical contribution ratio

The PCR of each mode is computed for all sensing nodes of the implemented sensor network on the Golden Gate Bridge. Figure 8 shows these ratios for the first four vertical modes. Similarly to the results of the numerical example, the PCRs are proportional to the modal ordinates. In addition, these ratios also depend on the modal amplitude factor (b) and modal frequency.

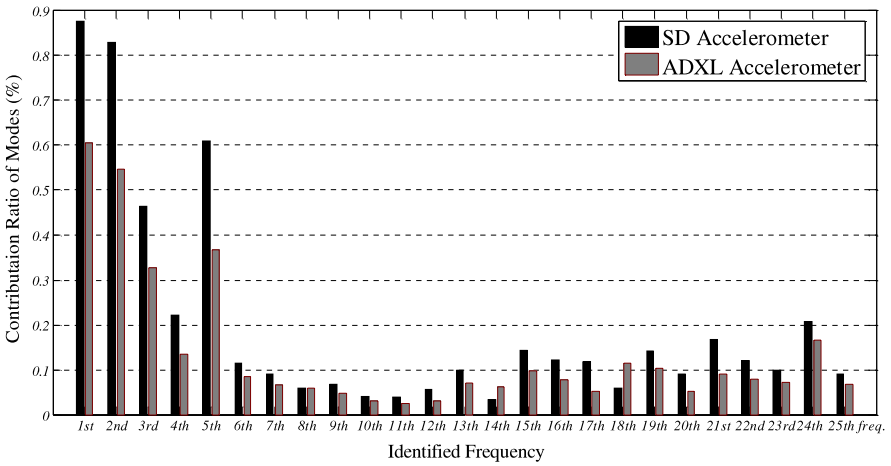

Figure 9. Overall physical contribution ratios of identified modes for 25 identified vertical modes.

Due to the long span of the bridge, many modes (with natural frequencies up to the Nyquist frequency) contribute in the measured response. Therefore, the contribution of each mode of vibration in the measured response is expected to be small. This is evident by comparing the amplitudes of the PCR values of this implementation with those of the 5 DOF simulated example.

Figure 8 shows that the Silicon Design 1221L, which has a lower noise level, presents a significantly higher PCR, compared to that of the ADXL202 sensors. This simply means that the noise contamination of the estimated impulse response is higher in the ADXL202 sensors and, therefore, the estimated modal parameters are more influenced by the measurement noise.

Although in theory higher modes usually have less participation in the response and therefore are more sensitive to the noise level, investigation of real data shows that some of the higher modes also have significant PCRs. This is reasonable since the ambient excitation does not necessarily have a perfectly constant spectrum and, therefore, some higher modes may be excited more than others. To observe the contributions of different modes in general, the PCRs of all the nodes are added together for each mode and plotted in figure 9. This Figure shows that the signal from the Silicon Design 1221L accelerometers has higher overall PCRs in almost all of the modes. At the same time, it can be realized that the difference is more significant for lower frequencies (e.g. the first five modes) rather than higher ones. This reflects the fact that the Silicon Design accelerometers are significantly more accurate than the ADXL accelerometers at low frequencies. This result highlights the importance of sensors with a low noise level at low frequencies for monitoring of long span bridges that have low fundamental natural frequencies.

6.4. Evaluation of the results using the MAC and MPC

The MAC and MPC are both evaluated for the identified modal parameters of the Golden Gate Bridge from the two networks of Silicon Design 1221L and ADXL202 sensors. Both of these parameters (MAC and MPC) were originally developed as tools to distinguish the structural modes from spurious ones. However, in this work, as accuracy indicators these parameters are used to evaluate and compare the accuracies of identified modes from two different sensor types.

Figure 10 shows the MAC and the MPC for 25 identified vertical modes. Comparing the results, it is clear that the network of Silicon Design sensors has resulted in more accurate modal parameters.

The low MAC and MPC values of the estimated results become more important when the selection of identified modes relies on these indicators. For example, the consistent mode indicator (CMI) is defined as the product of the MAC and the MPC (Pappa *et al* 1998) and is utilized in autonomous algorithms for selection of structural modes from spurious noise and/or computational modes (Pappa *et al* 1998, Nayeri *et al* 2009). The threshold for acceptance of identified modes suggested in these two articles is CMI greater than 80%. Figure 11 shows the values of this parameter for different identified modes for the two accelerometer types. It can be seen that many of the modes identified by ADXL202 sensors are not acceptable as accurate modes based on this criterion.

Generally, the results of identification for modes with lower frequency are less sensitive to the noise level, since the modal vibrations at those frequencies have higher amplitudes and, therefore, higher SNR in modal coordinates (as can be seen from the results of the previous section, (figure 9)). However, figure 11 shows that even in the low-frequency modes (third and fourth modes with frequencies of 0.17 and 0.21 Hz, respectively) identified by ADXL202 data the lack of confidence is evident. This is particularly reasonable as the ADXL202 sensors presented a high level of noise in the low-frequency range and probably the third and fourth identified modes from this sensor do not have enough amplitude to overcome the high noise of this frequency range.

7. Consistency of results through increase of the system's order

The last parameter which is evaluated in this study is the consistency of modal parameters through changes in the

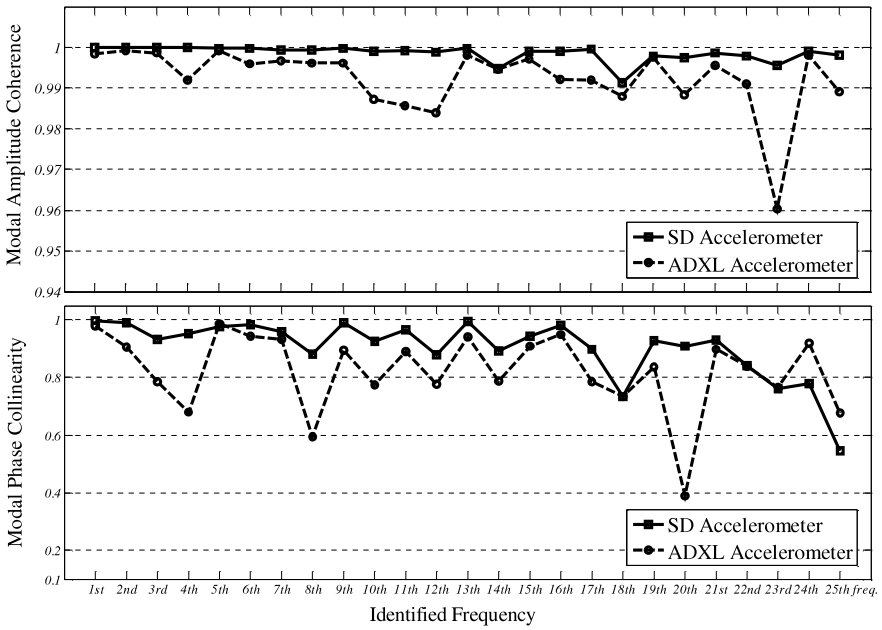

Figure 10. Modal phase collinearity and modal amplitude coherence of identified modes.

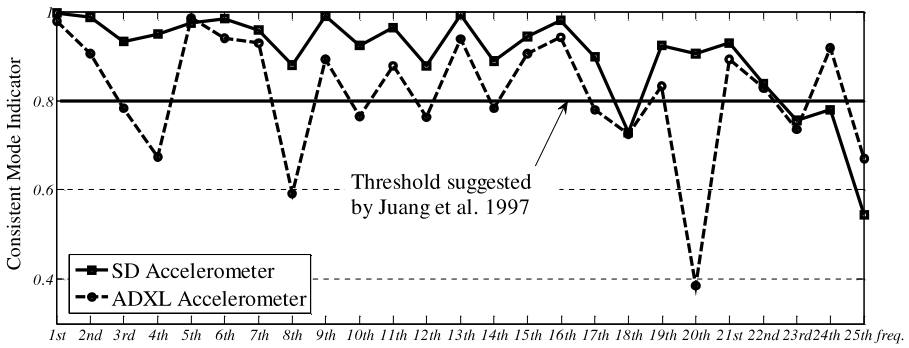

Figure 11. Consistency mode indicator of identified modes, using ERA–NExT.

system order. In the ERA process, the initial model order is usually selected higher than the desired number of modes to be identified. It is also conventional to use stabilization diagrams (Peeters and De Roeck 2001a) for selection of the model order which gives the most stable modal parameters. A difficulty associated with the selection of the model order is that the identified modal properties are not constant as the model order increases. This inconsistency is particularly significant for the case of damping ratios since the process of adding a pole into the system changes the damping ratios more than other parameters.

To detect the effect of measurement noise on the consistency of the modal parameters, the identified frequencies and damping ratios are inspected as the system's order increases. Figure 12 shows the frequencies in the 0.1–1.0 Hz range versus the selected system order for sensor networks with both ADXL202 and Silicon Design 1221L. Figures 13(a) and (b) also present the same information for the first five damping ratios, identified by the two different sensor types. The mean values and standard deviations of the identified damping ratios are also presented in the plots which help in comparing the consistency of results obtained from the two sensor types. For calculating the means and deviations of the results, the damping ratios outside the 0.5%–7.5% range are considered as outliers and excluded from this computation. Figure 13 shows that the sensors with lower noise level, Silicon Design 1221L, result in smaller deviations and are generally more consistent. However, the results for higher orders are fairly similar and stable for both systems. This means that increase of the model order and use of the stabilization diagram are quite effective in overcoming the inconsistency issue associated with identification of modal parameters.

8. Summary and conclusion

In this study, the influence of measurement noise on the accuracy and consistency of modal parameter identification is investigated. The physical contribution ratio (PCR) is developed to examine the level of contribution of physical modes in the estimation of impulse response. This parameter, PCR, is validated through implementation on a numerically simulated example and its behavior under the effects of

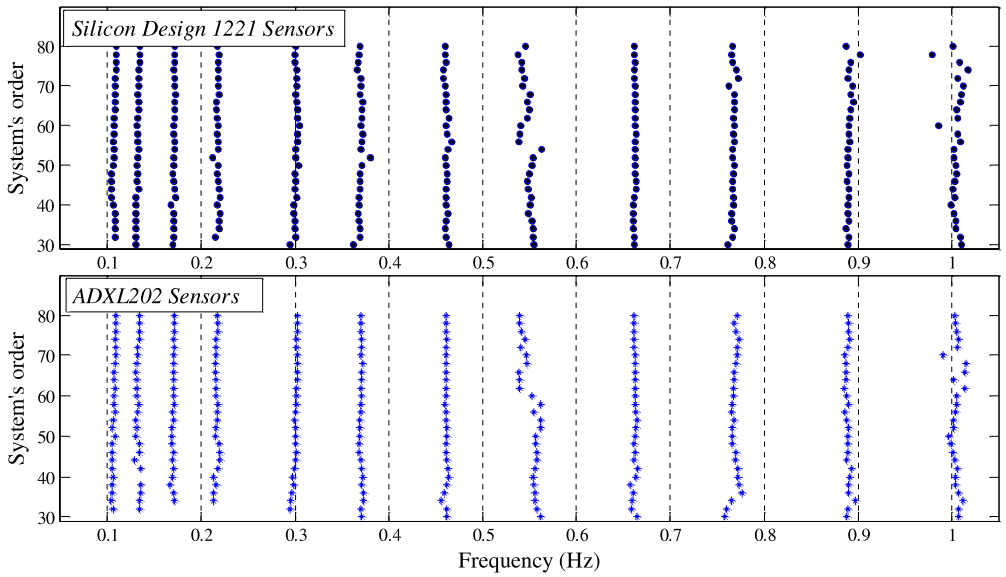

Figure 12. Consistency of the natural frequencies through increase of the model order.

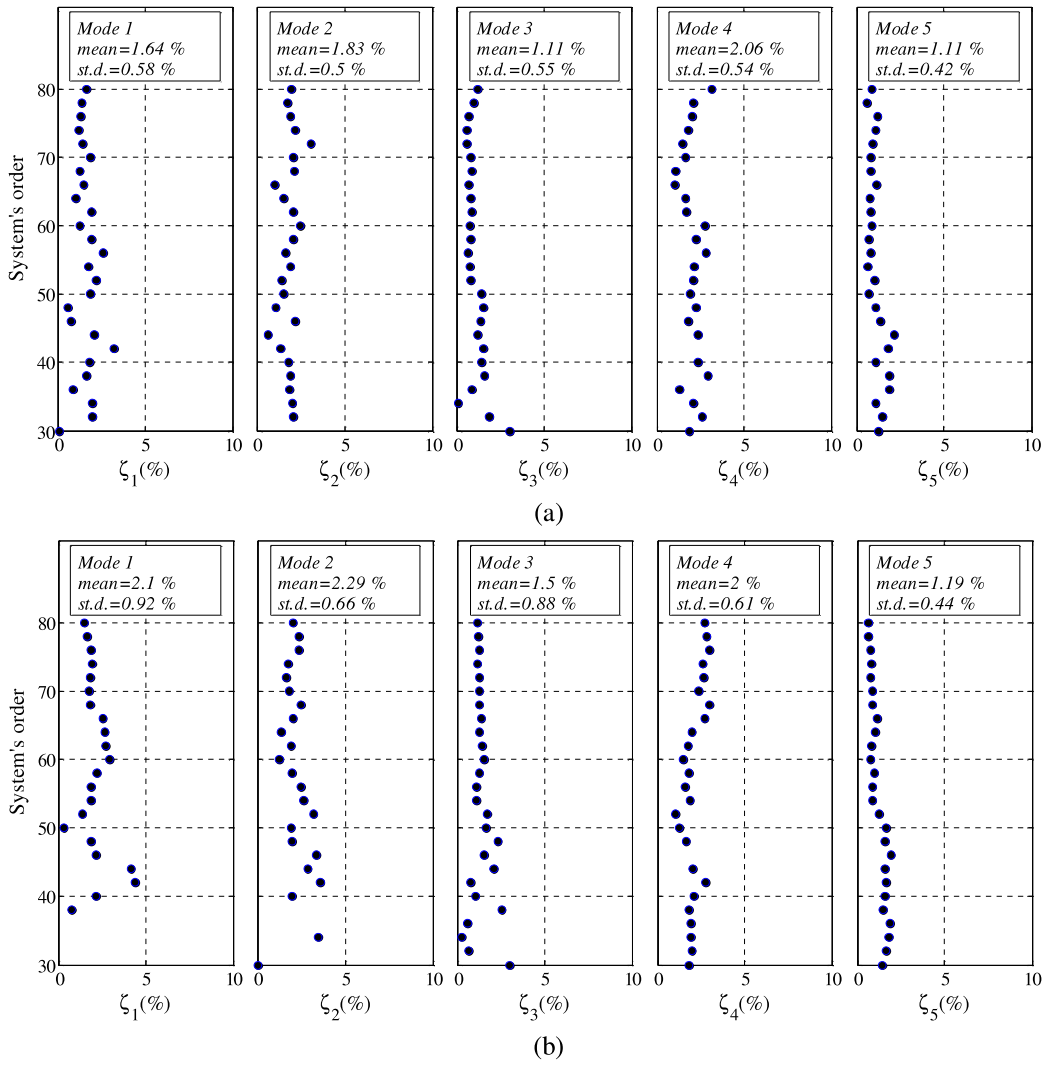

Figure 13. Consistency of the damping ratios through increase of the model order for (a) Silicon Design accelerometers and (b) ADXL201 accelerometers.

artificial noise and random structural changes is investigated. The PCR is also implemented on the ambient vibration data for the Golden Gate Bridge measured by two accelerometer sensors (ADXL 202 and Silicon Design 1221L) with different noise levels. To evaluate the effects of higher measurement noise, the modal parameters identified by the two sensor types are compared and inspected in terms of accuracy and consistency, using the presented parameter. The comparison of results obtained from the two sensor types showed a significantly higher PCR from the estimation using the low-noise sensor data. Furthermore, to quantify and compare the purity and accuracy of the modal parameters identified by the two measurement systems, modal amplitude coherence and modal phase collinearity are applied. The investigation shows higher purity in the results for low-noise accelerometer and failure of some modes identified by the ADXL202 accelerometer, based on an accuracy criterion. To detect the effect of measurement noise on the consistency of the modal parameters as the model order increases, the identified parameters (natural frequencies and damping ratios) are inspected throughout the increase of order, for the results of both sensor types. The results show that the deviation of the modal parameters obtained by the low-noise sensors is generally less than the deviation of the modal parameters identified by the sensors with higher noise level. However, the difference is not significant, particularly in higher model orders, and it can be concluded that the inconsistency of the results can be resolved by increasing the model order and through the use of a stabilization diagram.

While this work quantified the uncertainty of modal identification results associated with measurement noise, further studies are still needed to assess the uncertainty of results in the presence of both noise and environmental and operational changes.

References

Analog Devices 1999 ADXL202 low cost ±2 g dual axis iMEMS® accelerometer with duty cycle output www.analog.com/UploadedFiles/Data_Sheets/ADXL202E.pdf.

Beck J L, Vanik M W and Katafygiotis L S 1994 Determination of model parameters from ambient vibration data for structural health monitoring *Proc. 1st World Conf. on Structural Control (Pasadena, CA)* pp 3–12

Caicedo J M, Dyke S J and Johnson E A 2004 Natural excitation technique and eigensystem realization algorithm for phase I of the IASC-ASCE benchmark problem: simulated data *J. Eng. Mech.* **130** 49–60

Chung H C, Enotomo T, Loh K and Shinozuka M 2004 Real-time visualization of bridge structural response through wireless MEMS sensors *Proc. SPIE, Testing, Reliability, and Application of Micro- and Nano-Material Systems II* vol 5392 *(San Diego, CA)* pp 239–46

Farrar C R and James G H 1997 System identification from ambient vibration measurements on a bridge *J. Sound Vib.* **205** 1–18

Grimmelsman K A and Aktan A E 2005 Impacts and mitigation of uncertainty for improving the reliability of field measurements *Proc. 2nd Int. Conf. on Structural Health Monitoring of Intelligent Infrastructure (SHMII–2) (Shenzhen)*

James G H, Carne T G and Lauffer J P 1993 The natural excitation technique for modal parameter extraction from operating wind turbines *Rep. No. SAND92-1666, UC-261* (Sandia, NM: Sandia National Laboratories)

James G H, Carne T G, Lauffer J P and Nord A R 1992 Modal testing using natural excitation *Proc. 10th Int. Modal Analysis Conf. (San Diego)*

Jang S, Jo H, Cho S, Mechitov K, Rice J A, Sim S H, Jung H J, Yun C B, Spencer B F and Agha G 2010 Structural health monitoring of a cable stayed bridge using smart sensor technology: deployment and evaluation *Smart Struct. Syst.* **6** 439–59

Juang J N and Pappa R S 1985 An eigensystem realization algorithm for modal parameter identification and model reduction *J. Guid. Control Dyn.* **8** 620–7

Juang J-N and Pappa R S 1986 Effect of noise on modal parameters identified by the eigensystem realization algorithm *J. Guid. Control Dyn.* **9** 294–303

Kijewski-Correa T and Pirnia J D 2007 Dynamic behavior of tall buildings under wind: insights from full-scale monitoring *Struct. Design Tall Spe. Buildings* **16** 471–86

Kim J, Swartz R A, Lynch J P, Lee J J and Lee C G 2010 Rapid-to-deploy reconfigurable wireless structural monitoring systems using extended-range wireless sensors *Smart Struct. Syst.* **505–524** 505

Lynch J P 2006 A summary review of wireless sensors and sensor networks for structural health monitoring *Shock Vib. Dig.* **38** 91–128

Lynch J P, Law K H, Kiremidjian A S, Carryer E, Farrar C R, Sohn H, Allen D W, Nadler B and Wait J R 2004 Design and performance validation of a wireless sensing unit for structural monitoring application *Struct. Eng. Mech.* **17** 393–408

Lynch J P, Partridge A, Law K H, Kenny T W and Kiremidjian A S 2003 Design of piezoresistive MEMS-based accelerometer for integration with wireless sensing unit for structural monitoring *Aerosp.e Eng.* doi:10.1061/(ASCE)0893-1321

Lynch J P, Wang Y, Law K H, Yi J H, Lee C G and Yun C B 2005 Validation of a large-scale wireless structural monitoring system on the Geumdang Bridge *Proc. Int. Conf. on Safety and Structural Reliability (ICOSSAR) (Rome, June)*

Moon F L 2006 Impacts of epistemic (bias) uncertainty on structural identification of constructed (civil) systems *Shock Vib. Dig.* **38** 399–420

Nayeri R D, Tasbihgoo F, Wahbeh M, Caffrey J P, Masri S F, Conte J P and Elgamal A 2009 Study of time-domain techniques for modal parameter identification of a long suspension bridge with dense sensor arrays *J. Eng. Mech.* **135** 669

Overschee P V and Moor B D 1994 N4SID: subspace algorithms for the identification of combined deterministic-stochastic systems *Automatica* **30** 75–93

Pakzad S N 2010 Development and deployment of large scale wireless sensor network on a long-span bridge *Smart Struct. Syst.* **6** 525–43

Pakzad S N and Fenves G L 2009 Statistical analysis of vibration modes of a suspension bridge using spatially dense wireless sensor network *J. Struct. Eng.* **135** 863–72

Pakzad S N, Fenves G L, Kim S and Culler D E 2008 Design and implementation of scalable wireless sensor network for structural monitoring *ASCE J. Infrastruct. Eng.* **14** 89–101

Pandit S M 1991 *Modal and Spectrum Analysis: Data Dependent Systems in State Space* (New York: Wiley)

Pappa R S, Elliott K B and Schenk A 1993 Consistent-mode indicator for the eigensystem realization algorithm *J. Guid. Control Dyn.* doi:10.2514/3.21092

Pappa R S, James G H and Zimmerman D C 1998 Autonomous modal identification of the Space Shuttle tail rudder *J. Guid. Control Dyn.* **35** 163–9

Peeters B and De Roeck G 2001a Stochastic system identification for operational modal analysis: A review *J. Dyn. Syst., Meas., Control* **123** 659–67

Peeters B and De Roeck G 2001b One-year monitoring of the Z24-Bridge: environmental effects versus damage events *Earthq. Eng. Struct. Dyn.* **30** 149–71

Reynders E, Pintelon R and Deroeck G 2007 Uncertainty bounds on modal parameters obtained from stochastic subspace identification *Mech. Syst. Signal Process.* **22** 948–69

Reynolds P, Pavic A, Ibrahim Z and Street M 2004 Changes of modal properties of a stadium structure occupied by a crowd *Proc. IMAC XXII, Dearborn, DT, USA (January)*

Roeck G D, Claesen W and Broeck P V D 1995 DDS-methodology applied to parameter identification in civil engineering structures *Proc. Vibration and Noise* pp 341–53

Silicon Design 2007 Model 1221, low noise analog accelerometer www.silicondesign.com/pd.

Sohn H 2007 Effects of environmental and operational variability on structural health monitoring *J. Phil. Trans. R. Soc.* **365** 539–60

Straser E G and Kiremidjian A S 1998 *A Modular, Wireless Damage Monitoring System for Structures Technical Report 128* (Stanford, CA: John A Blume Earthquake Engineering Center, Stanford University)

Tanner N A, Wait J R, Farrar C R and Sohn H 2003 Structural health monitoring using modular wireless sensors *J. Intell. Mater. Syst. Struct.* **14** 43–56

Vold H and Rocklin G F 1982 The numerical implementation of a multi-input modal estimation method for mini-computers *Int. Modal Analysis Conf. Proc.*

Whelan M J and Janoyan K D 2009 Design of a robust, high-rate wireless sensor network for static and dynamic structural monitoring *J. Intell. Mater. Syst. Struct.* **20** 849–63